International Journal of Thin Films Science and Technology

http://dx.doi.org/10.18576/ijtfst/140306

Impact of Thickness, Work Function of Electrodes for Configuration of ($ZnO/Cs_2AgBi_{0.75}Sb_{0.25}$/ Spiro-OMeTAD) Perovskites Solar Cells

Murtadha J. Edam[1,], Fatimah Rabeea Jeji[1], Zainab Shiaa Kareem[1], Samir M. AbdulAlmohsin[1] and Hawraa M. Khadier[2]*

[1]Department of Physics, College of Education for Pure Sciences, University of Thi-Qar, Thi-Qar,64001, Iraq
[2]Department of Physics, College of Science, University of Thi-Qar, Thi-Qar, 64001, Iraq

Received: 22 May 2025, Revised: 2 Jun. 2025, Accepted: 3 Jul. 2025
Published online: 1 Sep. 2025

Abstract: In this study the findings indicated that the performance of lead-free perovskite solar cells was less adversely affected by elevated temperatures compared to lead-based solar cells, such as those utilizing lead perovskite $CH_3NH_3PbBr_3$. Lead-free perovskite solar cells have recently attained efficiency of around 18.23 percent. The conventional configuration of a perovskite-based planar heterogeneous solar cell comprises an electrode, a hole transport material (HTM), a perovskite absorber, an electron transport material (ETM), and a front electrode. This research presents ETM (ZnO) combined with perovskite $Cs_2AgBi_{0.75}Sb_{0.25}$ and Spiro-OMeTAD as the hole transport material (HTM) in an inorganic perovskite solar cell, achieving a high efficiency of 18.23% using SCAPS modeling. We investigate the impact of $Cs_2AgBi_{0.75}Sb_{0.25}$ layer thickness, varying from 0.1µm to 1µm, with optimal results seen at 0.1µm.

Keywords: Perovskites, simulation SCAPS, optimization efficiency, Solar Cells, temperature.

1 Introduction

The rising global energy demand, high costs, and harmful environmental effects from massive fossil fuel emissions provide substantial obstacles to the development of energy supply via traditional power generation. Solar cells and photovoltaic systems are proposed as solutions to renewable energy sources to mitigate these challenges. These devices convert sunlight into electrical energy, functioning as a sustainable and eco-friendly energy source. They are considered extremely promising and appropriate energy sources. Silicon-based photovoltaic devices dominate the solar cell market due to their availability, durability, and high power conversion efficiency (PCE) [1]–[10].

Nonetheless, the fabrication of an advanced silicone-based active layer entails substantial costs owing to the requirement for exceptionally high processing temperatures above 1400 °C, hence limiting its widespread commercialization. In recent years, hybrid organic-inorganic perovskite materials with the ABX3 structure, where A and B are monovalent and divalent metal cations, respectively, and X represents any halide, have been utilized by scientists in solar cell applications [10]–[14].

In 2016, a power conversion efficiency (PCE) of 21% was attained after seven years of development, in contrast to the initial 3.8% PCE reported in 2009, indicating a promising new generation of perovskite-based solar cells that are more cost-effective and simpler to produce than earlier solar cell generations [15], [16].

Moreover, solar cells utilizing perovskite materials derived from organic compounds and inorganic semiconductors exhibit straightforward chemical synthesis methods that facilitate precise adjustments of their optical and electronic characteristics [17]-[23].

The operational lifespan of organic perovskite compounds is constrained by heat instability caused by structural disintegration stemming from the volatile characteristics of the organic component, resulting in suboptimal performance of the photoelectric device. All inorganic perovskites have arisen as a potential method to enhance the thermal stability of photoelectric devices by substituting the organic cation at site A with an inorganic cation (Cs+). The totally inorganic perovskite-based photovoltaic device exhibits remarkable stability (90-95%) under ambient conditions at 25 °C, elevated temperatures (100 °C), and in the absence of encapsulation. Achieving high-performance perovskite solar cells is unnecessary. Among the several categories of inorganic perovskites, a-CsPbI3 has been predominantly investigated for photovoltaic applications owing to its optimal bandgap of 1.73 eV, which aligns effectively with the solar spectrum. Reviews emphasize the recent progress in perovskite solar cells employing CsPbI3 or CsSnI3 as the active material and Spiro-OMeTAD or PTA as the HTL for the cells' HTM. Although solar cells utilizing perovskite materials have attained power conversion efficiencies (PCE) exceeding 16%, the implementation of low-temperature processing

*Corresponding author E-mail: murtadhaj11@utq.edu.iq

remains economically unfeasible, primarily due to the high costs associated with polymeric materials like Spiro-OMeTAD or PTAA employed in the fabrication of hole transport materials (HTM).

Recent research has focused on perovskite solar cells (PSCs), particularly examining Spiro-OMeTAD as a P-type material, primarily as a hole transport material (HTM). This decision has diminished energy loss by decreasing interface recombination loss of electron-exciton couples in the Spiro-OMeTAD/perovskite cross-section. Moreover, Spiro-OMeTAD has enhanced mobility and facilitated superior perovskite crystallization on the HTL film. Perovskite solar cells employing Spiro-OMeTAD have exhibited advantageous performance regarding open-circuit voltage and elevated short-circuit current, resulting in improved energy conversion efficiency. This research examines the efficacy of inorganic perovskite materials, both lead-based and lead-free alternatives, as highly efficient light-absorbing sensor layers in solar cell applications.

We investigate the utilization of metal oxides, such as ZnO, as the ETL and Spiro-OMeTAD as the HTL. Additionally, we utilized lead-free perovskite Cs2AgBi0.75Sb0.25 as a layer for light absorption or photon harvesting. This study assessed the efficacy of solar cells constructed with lead compared to those fabricated without lead. The following sections examine and evaluate the results of photovoltaic devices.

2 Structure and working of perovskites

In the perovskite structures, which are typically written as ABX3, which X can be include nitrogen, carbon, oxygen, or a halogen, the A cation is located on octahedral place, and the B is cation placed on a cubooctahedral place (see Fig.1). Typically, B and A are anion and cation, respectively, when combined with an anion from O2. However, when halogen ions are present in the perovskite, monovalent and divalent ions can take up sites A and B.

As evident in Fig 2b, the A-position positive charge of cation in CH3NH3PbI3 is $CH3NH_3$+, while the B-place postion charge of Pb2+. The factor of geometric tolerance (t) is considered using the formula t = (rA + rX) / [√2(rB + rX)] and is used to determine the perovskite's potential for formation. Here, the radii of the A, B, and X ions are represented by rA, rB, and rX, respectively. Forovskites that contain cations that transition to metal and oxide, a t value of 1 represents the ideal cubic formation of perovskites, while a t value of less than 1 suggests that the structure is octahedralized [15] .

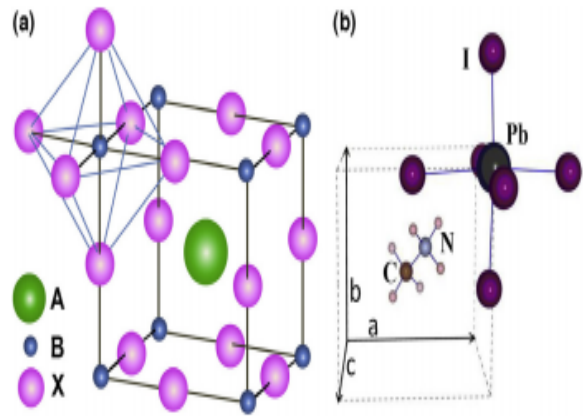

Fig. 1: (a) ABX_3 perovskite configuration with large A cations on BX6 octahedra and cuboctahedrons. (b) Cubic perovskite unit cell CH3NH3PbI3. The inventive numbers in-b-were copied [16].

The perovskite film first receives number of photon, thereby producing exciton. Due to exciton energy inequality inside perovskite material, the materials emit free electrons or holes to create current [25-28]. Longer propagation distance and carrier lifetime are the basis for the higher performance of solar energy base perovskits Tenth. Electron-hole pairs separate ZnO/perovskite, ZnO/perovskite with the two heterojunction, injected electrons into ZnO/perovskite, and then inject electrons into ZnO during the injection process (process in Fig 3). (i)), inject holes (ii).) High temperature TM.) realizes charge transfer [29]. Additionally, various behaviors influence the efficiency of the cell, such as the exciton extermination procedure (iii), recombination and photoluminescence, and turn around movement of holes and electrons (processes (iv) and (v), for recombination and generation. may give. **ZnO**/ETM interfacial process (vi). Figure 2 shows the electron transfer in HTM/perovskite/ ZnO cell.

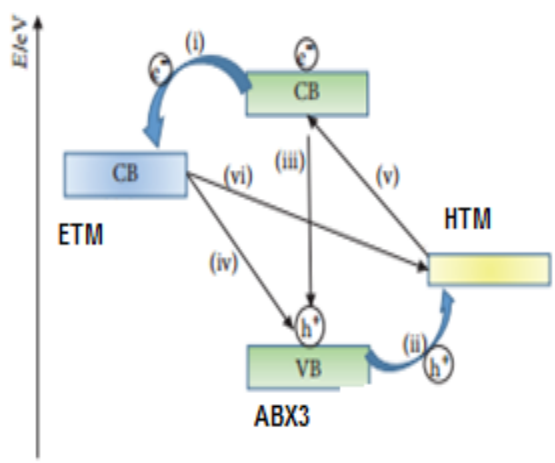

Fig. 2: Diagram of energies of materials and processes transport of electrons and holes in the structure[30].

Burgelman led to development of SCAPS1D software. Simulation the electronics properties of device solar cell with a diode by solve the fundamental mathematical relation of solar cells in a consistent state [31]. In this structure, it employed to investigate the actual device with different materials properties in order to improve its effectiveness. The program allows for the addition of extra and interface that are non-reactive. Many of the loss of recombination in the considered system are attributed to radiation (e.g. recombination act directly from band to band) and interface recombination. The flow diagram beneath describes the steps involved in attempting to simulate using SCAPS.

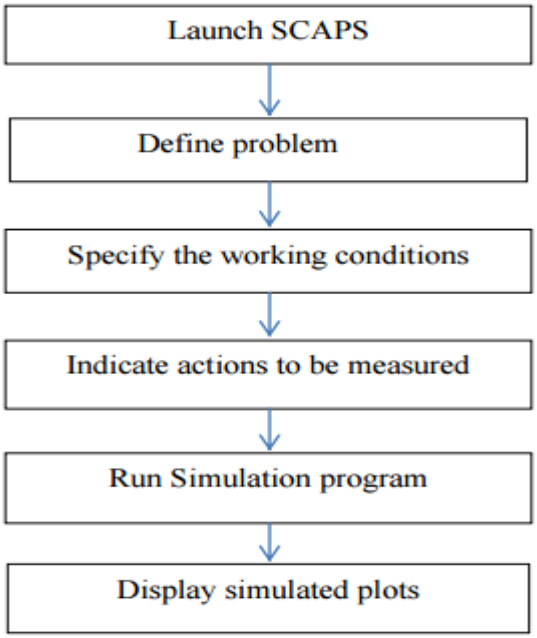

Fig. 3: simulation procedure

3 Numerical SCAPS Simulations

Simulation is essential to gaining sympathetic of physical activities, potential success of projected physical explanations, in addition to the consequences of physical natural changes to solar cell act. Several models of simulation are employed to simulate solar cells such as AMPS, SCAP, etc. SCAPS is model program that has seven different layers of semiconductor designed by a group of researchers that specialize in solar cells at the Department of Systems Electronics devices at the Ghent University in Belgium [32]. Creating solar-powered cells lacking associated projects is futile and time-consuming. It analyses the properties of each layer and their purpose in order to maximize the power conversion efficiency of the solar cell. To emulate a PC, every necessary input parameter must be accurately specified for it to purpose as a computer. A legitimate complement. Perovskite solar cells have a different devise than others like CIGS thin film, and perovskites are composed of interesting shapes called Vanier. As a result, SCAPS can be employed as a one-dimensional model of perovskite-based solar cells [25].

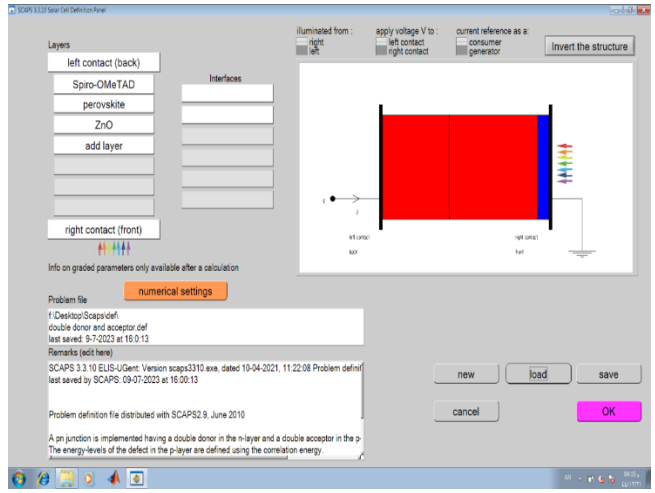

Fig. 4: Pane for layer properties of SCAPS.

Voltage Φ and charge q are related to Poisson's equation:

$$\frac{\partial^2}{\partial x^2}\varphi(x) = \frac{q}{\varepsilon}[n(x) - p(x) - N_D^+(x) + N_A^-(x) - P_t(x) + n_t(x)] \quad (1)$$

where the basic charge q, the permittivity ε, the free electron density n(x), the free hole density p(x), the ionized donor-like injecting density $N_D^+(x)$, ionized acceptor-like injecting density $N_D^+(x)$, the bound hole density pt(x), and the confined electron density nt(x). the equations for the continuation of electrons and holes:

$$q\frac{\partial n}{\partial t} = \frac{\partial J_n}{\partial t} + qG - qR \quad (2)$$

$$q\frac{\partial p}{\partial t} = -\frac{\partial J_p}{\partial t} + qG - qR \quad (3)$$

$$J_n = qn\mu_n\frac{\partial \varphi}{\partial x} + qD_n\frac{\partial n}{\partial x} \quad (4)$$

$$J_p = qp\mu_p\frac{\partial \varphi}{\partial x} + qD_p\frac{\partial p}{\partial x} \quad (5)$$

[33,34].

4 SCAPS model of ZnO /Perovskite semi-conductor / Spiro-OMeTAD

It's important to note that all of the parameters associated with every layer in the device are derived from reported data from experimental, these sources include [35]. Table 1 include the main parameters employed the simulations.

Table 1: substance parameter of ETM, HTM, and absorber [36-39].

Parameters	Spiro-OMeTAD	Perovskite	ZnO
Band gap(ev)	2.9	1.8	3.3
Electron effinity (ev)	2.2	3.58	4.0
Dielectric permittivity	3	6.5	9.0
CB effective density of states (1/cm^2)	2.50X10^{18}	2.2 × 10^{18}	3.7 × 10^{18}
VB effective density of states (1/cm^2)	1.80X10^{19}	1.8 × 10^{19}	1.8 × 10^{19}
Electron mobility (cm^2/v.s)	2.00X10^{-04}	2	100

Hole mobility (cm^2/v.s)	$2.00X10^{-04}$	2	25
electron thermal velocity (cm/s)	1.00×10^7	$1.00x10^7$	$1.00x10^7$
hole thermal velocity (cm/s)	$1.00x10^7$	$1.00x10^7$	$1.00x10^7$

5 Result and Discussion

5.1 Thickness of absorber layer

The layer of material that absorbs photons must possess an ideal thickness to generate the maximum number of hole-electron pairs by the absorption of the highest possible quantity of photons. The thickness of the perovskite layer has been altered from 0.1 µm to a final measurement of 1 µm. When the thickness of the perovskite layer increases, the probability of charge carriers (electrons and holes) recombining prior to reaching the charge extraction layers also escalates. This is particularly crucial for thick layers, as the carriers may not diffuse rapidly enough to reach the electrodes prior to recombination, hence diminishing efficiency.[40]. The peak efficiency is 17.75% at a thickness of 0.1 µm, which corresponds to the optimal light absorption level.

Table 2: Variant of Thickness for $C_{s_2}AgBi_{0.75}Sb_{0.25}Br_6$ with solar cells parameters.

Thickness (µm)	V_{oc}(V)	J_{sc}(mA /cm^2)	F.F (%)	η (%)
0.1	1.3683	25.773404	50.34	17.75
0.2	1.3523	17.066630	47.68	11.00
0.3	1.3491	14.546662	49.21	9.66
0.4	1.3485	14.091578	49.61	9.43
0.5	1.3485	14.016050	49.67	9.39
0.6	1.3484	14.007053	49.68	9.38
0.7	1.3484	14.009490	49.67	9.38
0.8	1.3484	14.013599	49.67	9.39
0.9	1.3484	14.017670	49.66	9.39
1	1.3484	14.021442	49.66	9.39

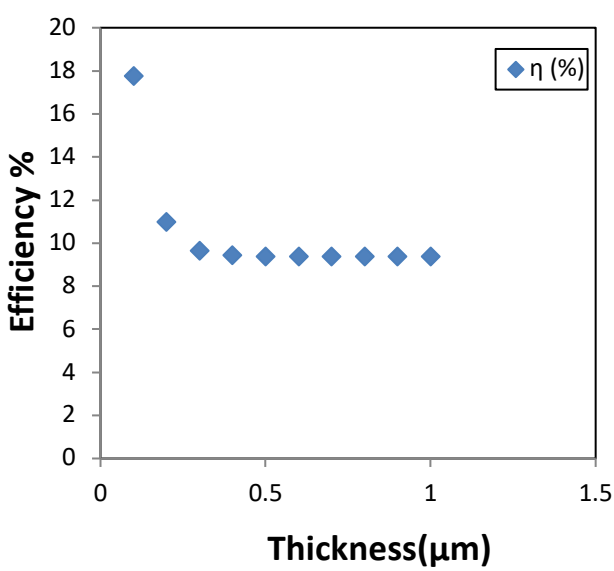

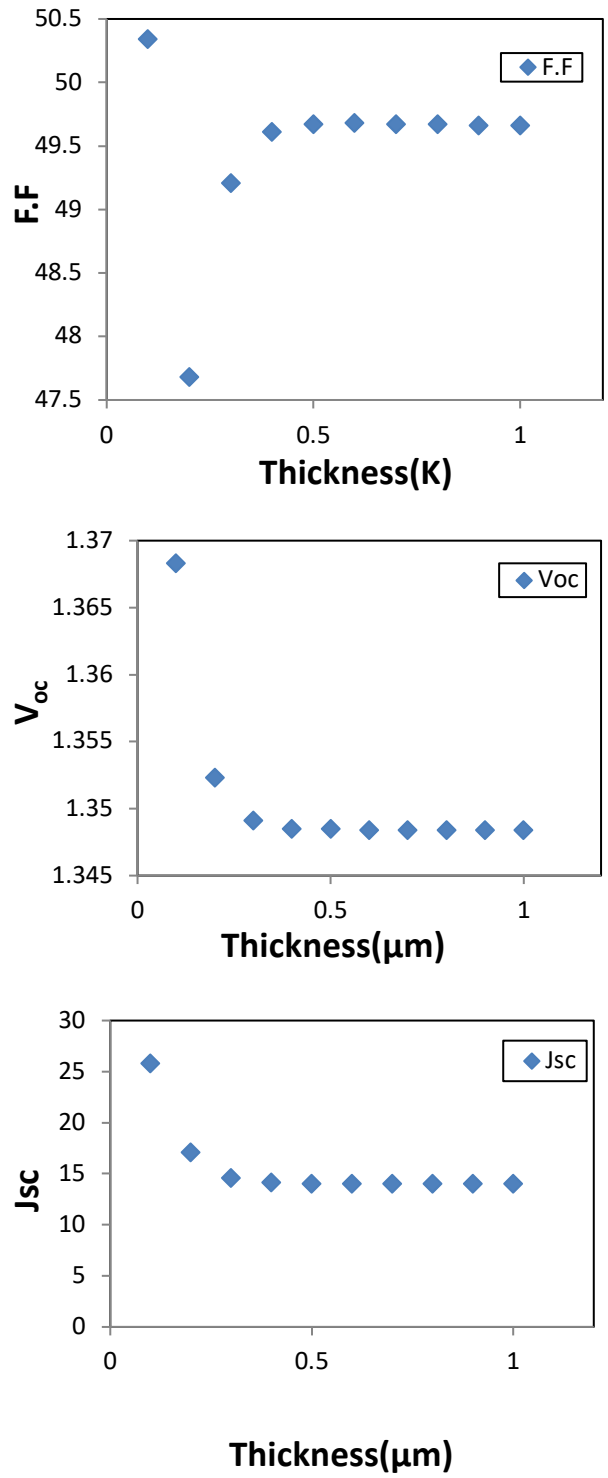

Fig. 5: Variant of parameters of solar cells by changeable the thickness of $C_{s_2}AgBi_{0.75}Sb_{0.25}$.

5.2 Thickness of ZnO layer

An optimally configured ETL thickness guarantees effective electron extraction and transport, minimizing recombination losses. Insufficient ETL thickness may result in inadequate covering of the perovskite layer, leading to

suboptimal electron collection and heightened recombination. The thickness of the ZnO layer has been modified from 0.01 µm to 0.09 µm, whereas the open-circuit voltage (Voc) exhibits a minimal drop contingent upon the intensity of light incident on the solar cell. The peak efficiency is 17.75% at an overall thickness of 0.09 µm.

Table 3: Variation of Thickness for ZnO (n) with device parameters.

Thickness (µm)	V_{oc}(V)	J_{sc}(mA /cm^2)	F.F (%)	η (%)
0.01	1.3686	25.005145	40.53	14.89
0.02	1.3685	25.377266	41.85	15.11
0.03	1.3685	25.537994	44.78	15.94
0.04	1.3684	25.593650	47.58	16.76
0.05	1.3684	25.745139	49.39	17.30
0.06	1.3684	25.851457	50.32	17.58
0.07	1.3683	26.561703	50.62	17.70
0.08	1.3683	26.647319	50.57	17.75
0.09	1.3683	26.773404	50.34	17.75

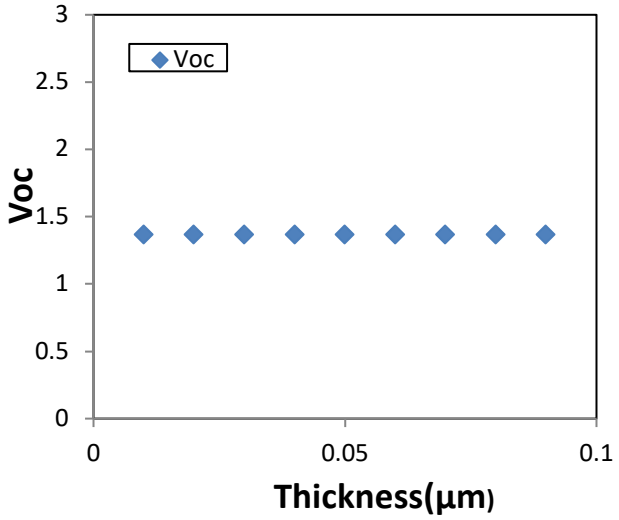

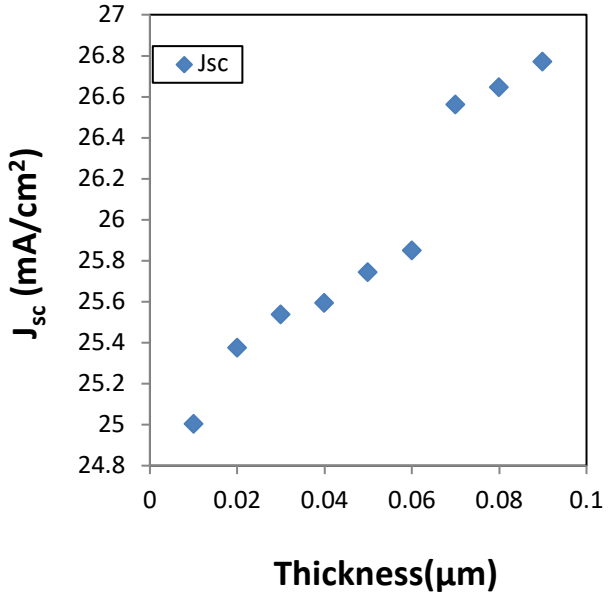

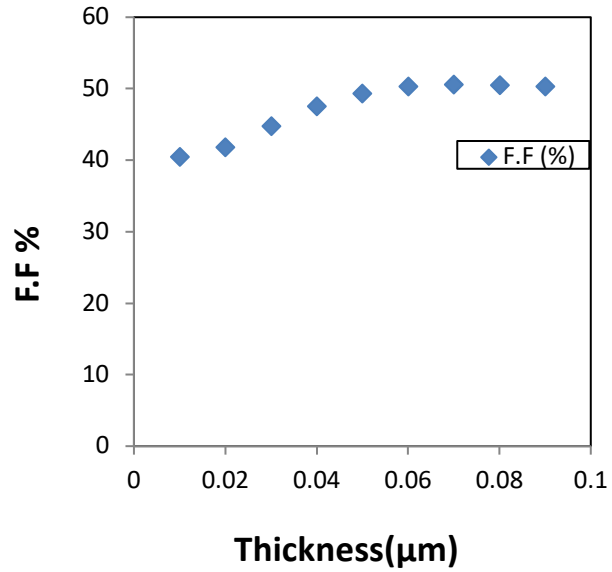

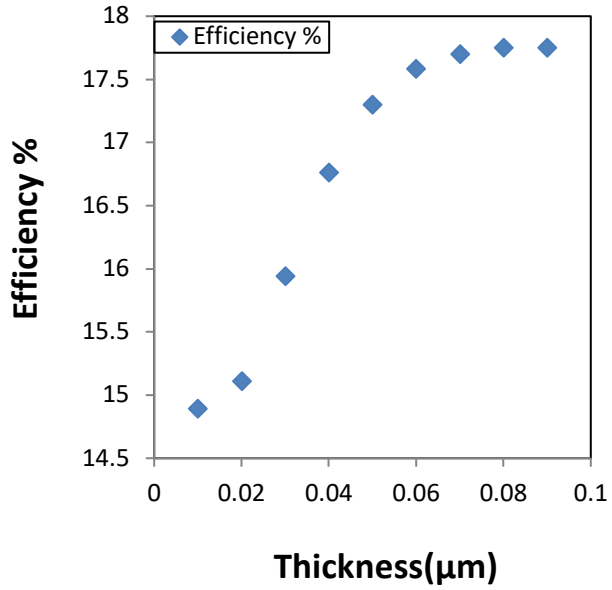

Fig. 6: Difference parameters of device by tunable the thickness of ZnO.

5.3 Thickness of SpiroOMeTAD layer

Modifying the thickness of the hole transport layer (HTL) in (PSCs) influences optical effects and light absorption. Thinner HTL can influence light absorption in the perovskite layer. Increased thickness of the HTL facilitates enhanced light penetration to the perovskite absorber, which may lead to improvements in Jsc and overall efficiency. The thickness of the Spiro-OMeTAD layer has been modified within the range of 0.01 µm to 0.1 µm. Increased film thickness results in significant electron-hole production. Figure 7 illustrates. The open-circuit voltage remains constant despite an increase in thickness. As the short circuit current increases, the results indicate an ideal efficiency of 17.34% at 0.1 µm.

Table 4: Variation of Thickness for Spiro-OMeTAD with device parameters.

Thickness (μm)	V_{oc}(V)	J_{sc}(mA /cm^2)	F.F (%)	η (%)
0.01	1.3570	15.015618	54.04	11.01
0.02	1.3630	20.022632	51.84	14.15
0.03	1.3652	22.331892	51.15	15.60
0.04	1.3662	23.389359	50.88	16.26
0.05	1.3667	23.984214	50.74	16.63
0.06	1.3670	24.365699	50.65	16.87
0.07	1.3673	24.633186	50.59	17.04
0.08	1.3675	24.832961	50.54	17.16
0.09	1.3676	24.989194	50.51	17.26
0.1	1.3677	25.115681	50.48	17.34

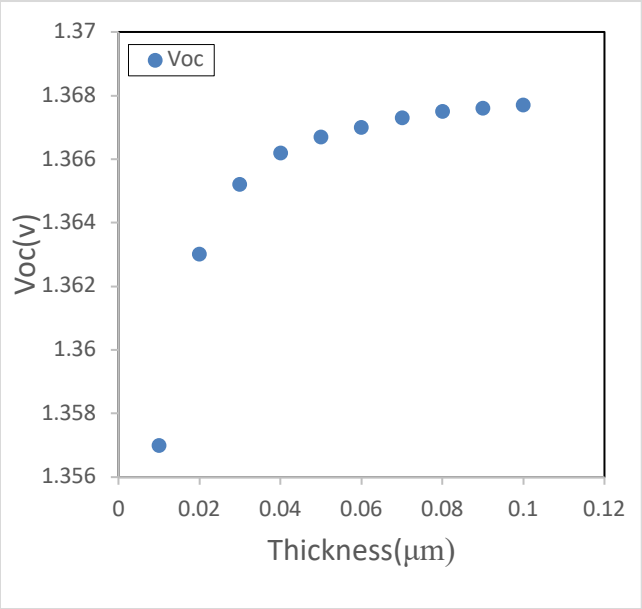

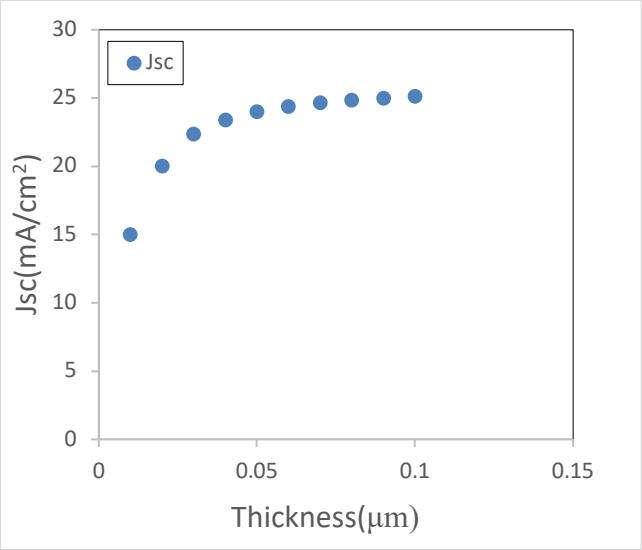

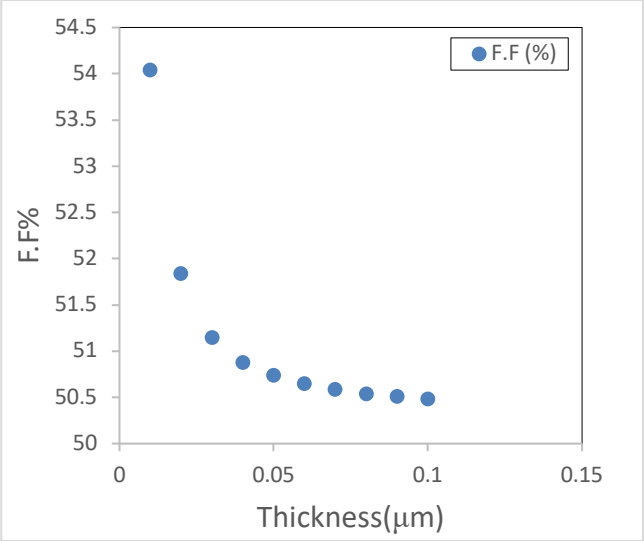

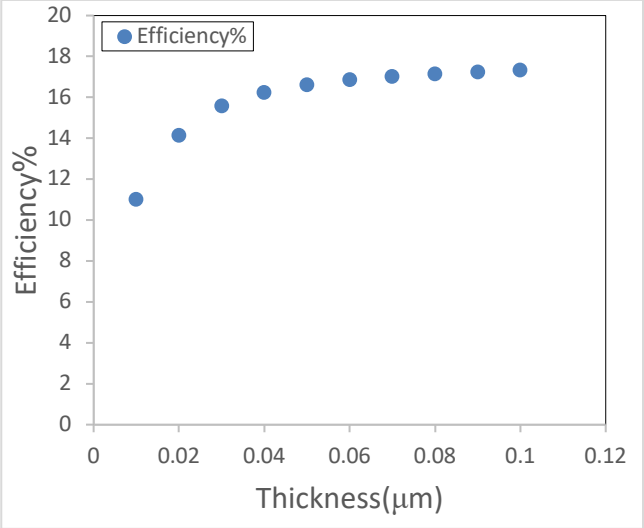

Fig. 7: Difference of solar cells measurement by changing the thickness layer of Spiro-OMeTAD.

5.4 Effect of annealing Temperatures

The outcomes of the simulation involving I-V characteristics, including FF, PCE, Jsc, and Voc of solar cell devices at various environmental temperatures, are presented in Table 2, where Jsc = 26.280830 mA/cm², FF = 54.07, and the maximum efficiency is 18.23%. Optimal efficiency occurs at a temperature of 355 K, coinciding with the temperature at which the cell exhibits optimum stability. As the temperature rises from 350 K to 500 K, the formation of electron-hole pairs in the perovskite material diminishes, resulting in a decrease in PCE, Voc, and Jsc, . Figure 8 illustrates that the open circuit voltage diminishes gradually as the temperature rises. The effectiveness of solar cells can be modified by temperature through the regulation of carrier generation, collection, and recombination; thus, the best temperature for perovskite solar devices utilizing ZnO in their photovoltaic solar cells is 350 K.

Table 5: The factors of the Spiro-OMeTAD (P)/ $C_{s_2}AgBi_{0.75}Sb_{0.25}Br_6$ / ZnO(n) heterojunction solar cells.

Temperature (K)	V_{oc}(V)	Jsc (mA/cm^2)	F.F (%)	η (%)
100	1.1942	26.473759	57.50	18.18
150	1.1942	26.473759	57.50	18.18
200	1.1942	26.473759	57.50	18.18
250	1.1942	26.473759	57.50	18.18
300	1.3683	25.775154	50.35	17.76
350	1.2828	26.280830	54.07	18.23
400	1.1942	26.473759	57.50	18.18
450	1.1034	26.568508	60.85	17.84
500	1.0105	26.614826	63.53	17.09

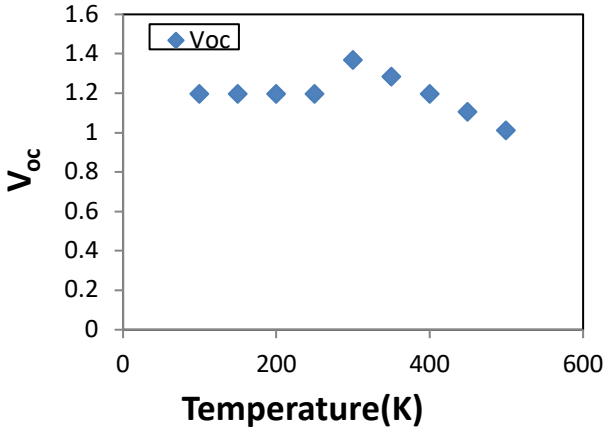

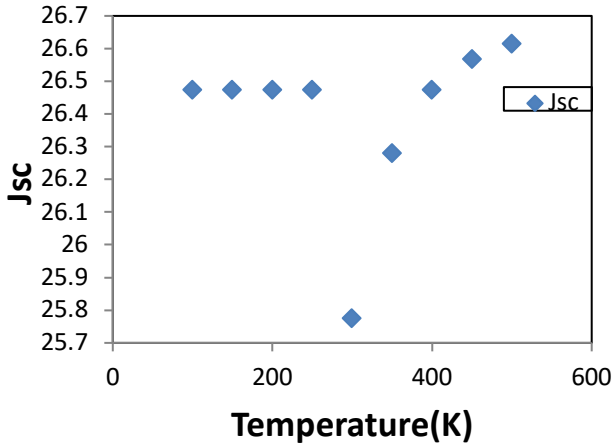

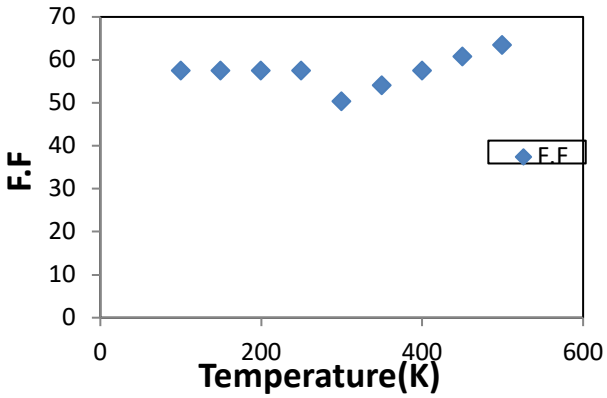

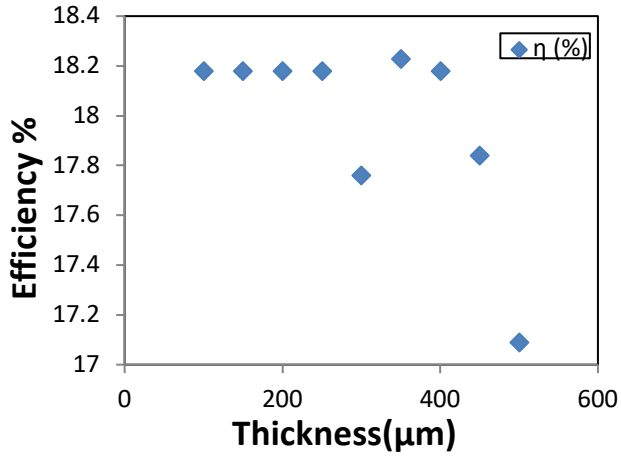

Fig. 8: The variation of solar cell parameters with the temperature.

5.5 Effect of Different Back Contacts as electrodes

Solar cells with back contacts made of Cr, Si, Ag, Ta, and Ni were simulated. As seen in Figure 9, varying degrees of rear contact power have varied impacts. Voc, Jsc, and FF volumes will rise in tandem with the expansion of the foil matter business. This also improves the performance of perovskite solar cells. It is energetically unfavorable to travel towards the electrode because the electric field at the HTM/back contact is negative [41]. According to the simulation results, Ta has the ability to improve the performance of PSCs.

Table 6: shows the effect of various metal back contact on the parameters of solar cells.

Metals	Work Function (ev)	V_{oc}(V)	J_{sc}(mA/cm^2)	F.F (%)	Efficiency %
Cr	4.5	1.2103	25.797045	49.40	15.42
Si	4.6	1.2782	26.105157	51.58	17.21
Ag	4.7	1.2826	26.262263	53.83	18.13
Ta	4.8	1.2828	26.279995	54.06	18.23
Zn	4.9	1.2828	26.280793	54.07	18.23

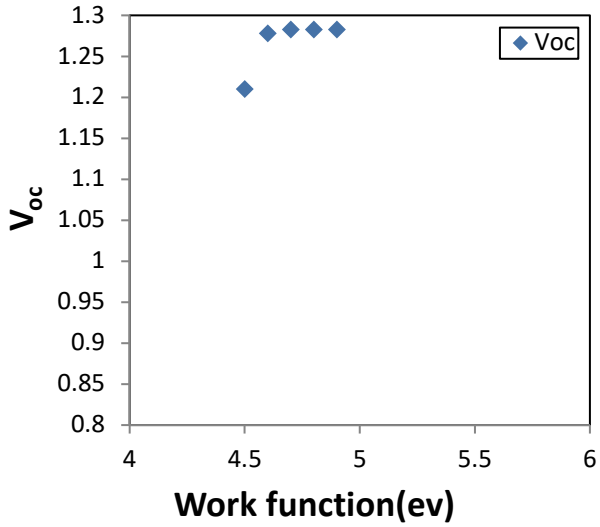

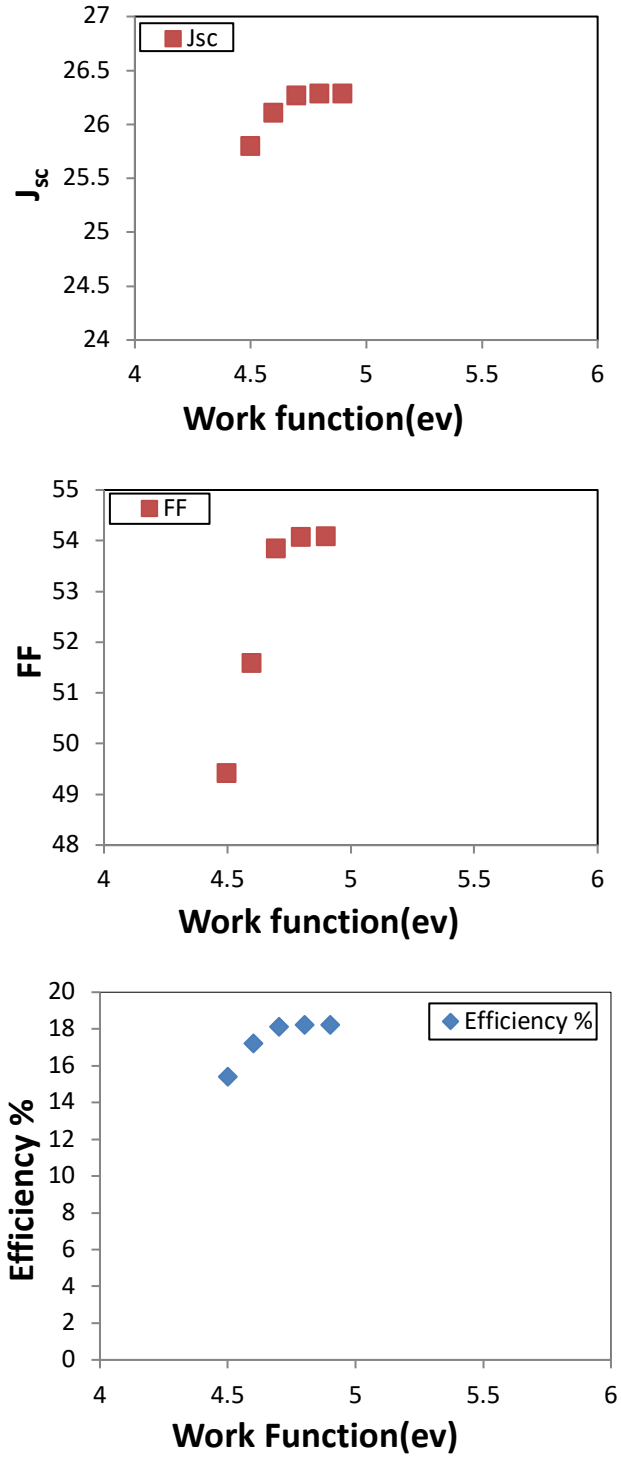

Fig. 9: Work function values of metals versus Voc, Jsc, FF and η%.

5 Conclusions

1. If thickness of $Cs_2AgBi_{0.75}Sb_{0.25}Br_6$ layer is increased, the power conversion efficiency, Jsc ,Voc with F.F are decreased, due to the low amount of radiation reaching the active layer.
2. An ideal power conversion efficiency (PCE) of 18.23% may be achieved by combining work function equal to 4.8 ev.
3. The recombination of the produced photo-electrons and holes via the electrode can be prevented by the SPIRO-OMeTAD layer which acts as a barrier potential between the perovskite layer and the electrode.

Reference

[1] Z. R. Abdulsada, S. B. Kadhim, S. M. AbdulAlmohsin, and H. S. Abdulaali, "High Efficiency (22.46) of Solar Cells Based on Perovskites," *University of Thi-Qar Journal of Science*, vol. 10, pp. 187-191, 2023.

[2] Z. R. Abdulsada and S. M. AbdulAlmohsin, "High Efficiency Solar Cells Base on Organic-inorganic Perovskites Materials," *University of Thi-Qar Journal of Science*, vol. 8, pp. 23-29, 2021.

[3] A. A. Hussein, "Enhancement Efficiency of Active Layer P3HT: POT: DBSA/PCBM Photoactive Solar Cell Device," *University of Thi-Qar Journal of Science*, vol. 7, pp. 90-94, 2020.

[4] M. J. Edam, S. M. AbdulAlmohsin, D. A. Bilal and M. O. Oleiw "Highest Efficiency of Perovskite Structure Solar Cells," Int. J. Thin Film. Sci. Technol., vol. 13, no. 1, pp. 1–10, 2024.

[5] M. J. Edam, S. M. Abdulalmohsin, H. M. Khadier, B. H. Auad, and D. E. Tarek, "Defect and Thickness Optimization of Perovskite for High Efficiency Solar Cells," *Defect Diffus. Forum*, vol. 433, pp. 27–37, 2024.

[6] Z. Raheem, Zainab. R. Abdulsada, Sally Basim Kadhim, Samir M. AbdulAlmohsin, and Hayder Saadoon Abdulaali, "High Efficiency (22.46) of Solar Cells Based on Perovskites," *Univ. Thi-Qar J. Sci.*, vol. 10, no. 2, pp. 187–191, 2023.

[7] S. M.AbdulAlmohsin and D. E.Tareq, "Fabrication and simulation of peroviskite solar cells comparable study of CuO and Nano composite PANI/SWCNTS as HTM," *AIMS Energy*, vol. 8, no. 2, pp. 169–178, 2020.

[8] H. A. Rshash and S. M. Abdul Almohsin, "Optimization of Thickness, Energy Band Gap, and Temperature for High Efficiency of Lead Halide Perovskite Solar Cell," *Int. J. Thin Film Sci. Technol.*, vol. 13, no. 3, pp. 225–233, 2024.

[9] D. E. Tareq, S. M. Abdulalmohsin, and H. H. Waried, "Perovskite solar cells based on CH3NH3SnI3Structure," *IOP Conf. Ser. Mater. Sci. Eng.*, vol. 928, no. 7, 2020.

[10] M. J. Edam, A. S. Mahdi, S. M. Abdulalmohsin,

and H. M. Khadier, "Perovskites Solar Cells Study Optimization Thickness, Temperature and Work Function," *J Nanostruct*, vol. 15, no. 3, pp. 1208–1219, 2025, doi: 10.22052/JNS.2025.03.038

[11] S. Zhu, X. Yao, Q. Ren, C. Zheng, S. Li, Y. Tong, B. Shi, S. Guo, S. Fan, L. Ren, H.; et al. Transparent electrode for monolithic perovskite/silicon-heterojunction two-terminal tandem solar cells. *Nano Energy* **2018**, *45*, 280–286. [CrossRef]

[12] S. Hadi and A. H. Al-Khursan, "Developing The Performance of Double Quantum Dot Solar Cell Structure," *University of Thi-Qar Journal of Science*, vol. 8, pp. 148-154, 2021

[13] E. T. McClure, M.R. Ball, Windl, W. Woodward PM. Cs2AgBiX6 (X = Br, Cl): New Visible Light Absorbing, Lead-Free Halide Perovskite Semiconductors. *Chem. Mater. Am. Chem. Soc.* **2016**, *28*, 1348–1354.

[14] A. M. Jafar, K. A. Khalaph, A. M. Hmood, and N. K. Abdalameera, "Pb-Free metal halide double perovskite, Cs2SbAgX6, X = i or Cl, with TiO2 nano-particles in solar cell applications," *AIP Conf. Proc.*, vol. 2834, no. 1, 2023.

[15] A. M. Jafar, K. A. Khalaph, A. M. Hmood, and N. K. Abdalameera, "Pb-Free metal halide double perovskite, Cs2SbAgX6, X = i or Cl, with TiO2 nano-particles in solar cell applications," *AIP Conf. Proc.*, vol. 2834, no. 1, 2023.

[16] J. Madan, R. Shivani Pandey, R. Sharma, Device simulation of 17.3% efficient lead-free all-perovskite tandem solar cell. *Sol. Energy* **2020**, *197*, 212–221. [CrossRef]

[17] S. Cell and C. Efficiency, "Device Optimization of a Lead-Free Perovskite/Silicon Tandem Solar Cell with 24.4% Power Conversion Efficiency," *Energies* . **2021**,14 (12), 3383; https://doi.org/10.3390/en14123383

[18] H. M. Khadier, H. B. Al Husseini, and A. M. Jafar, "An Analysis Comparing The Performance Of Lead And Tin Halides In Organic Perovskite Materials CH3NH3 PbxSn1-xI3, Where x = 1, 0.5, or 0, For Use In Solar Cells," *J. Opt.*, 2024.

[19] H. mohammed khadier, H. B. Al Husseini, and A. Mashot Jafar, "An analysis comparing the performance of lead and tin halides organic Perovskite Solar Cells and numerical simulation with SCAPS," *Opt. Mater. (Amst).,* vol. 155, no. April, p. 115814, 2024.

[20] A. M. Jafar, F. M. Al-Attar, K. I. Inad, A. M. Hmood, S. M. Saleh, and K. A. Khalaph, "Preparation and simulation of lead mix-halide perovskite solar cells," *AIP Conf. Proc.*, vol. 2213, no. March, 2020.

[21] Zainab. R. Abdulsada and Samir M . AbdulAlmohsin, "High Efficiency Solar Cells Base on Organic-inorganic Perovskites Materials," *Univ. Thi-Qar J. Sci.*, vol. 8, no. 2, pp. 23–29, 2021.

[22] H. K. Mejbel, "Study the Defect of Organic Electron Transport Materials of Perovskites Solar Cell Study the Defect of Organic Electron Transport Materials of Perovskites Solar Cell," *Int. J. Thin Film. Sci. Technol*, vol. 12, no. 3, 2023.

[23] A. M. Jafar, K. A. Khalaph, and H. B. Al Husseini, "Study of the structural , electronic , mechanical , electro-thermal and optical properties of double perovskite structures Cs 2 SbAgX 6 , (X = I , Br , or Cl)," *Phys. Scr.*, vol. 97, no. 8, p. 85509, 2022.

[24] C. Series, "Quantum Dotes of Perovskites Solar Cells based on ZnSe as ETM Quantum Dotes of Perovskites Solar Cells based on ZnSe as," *J. Phys. Conf. Ser.*, 2021.

[25] D. E. Tareq, M. J. Edam, H. M. Khadier and S. M. Abdulalmohsin, "THE BEST EFFICIENCY OF ORGANIC-INORGANIC QUANTUM DOTPEROVSKITE SOLAR CELLS," *Int. J. Curr. Res.*, vol. 16, no. 6, pp. 28822–28829, 2024.

[26] M. Rini, et al. Nature 449 (2007) 72–74.

[27] G. Giorgi, et al. J. Phys. Chem. Lett. 4 (2013) 4213–4216.

[28] M. A. Green, A. Ho-Baillie, and H. J. Snaith, "Te emergence of perovskite solar cells," *Nature Photonics*, vol. 8, no. 7, pp. 506–514, 2014.

[29] S. P. Singh and P. Nagarjuna, "Organometal halide perovskites as useful materials in sensitized solar cells," Dalton Transactions,vol. 43, no. 14, pp. 5247–5251, 2014

[30] A. Marchioro, J. Teuscher, D. Friedrich et al., "Unravelling the mechanism of photoinduced charge transfer processes in lead iodide perovskite solar cells," Nature Photonics, vol. 8, no. 3, pp.250–255, 2014

[31] D. Zhou, T. Zhou, Y. Tian, X. Zhu, and Y. Tu, "Perovskite-Based Solar Cells: Materials, Methods, and Future Perspectives," *J. Nanomater.,* vol. 2018, 2018, doi: 10.1155/2018/8148072.

[32] Burgelman et al, SCAPS manual, no. May. 2014.

[33] Niemegeers A, Burgelman M, Decock K. SCAPS Manual. University of Gent. 2014.

[34] T. Minemoto, M. Murata, "Device modeling of perovskite solar cells based on structur-al similarity with thin film inorganic semiconductor solar cells," Journal of Applied Physics. 2014;116: 5, 054505.

[35] Amu, Tochukwu Loreta , Dr. Akin-Ojo Omololu,

Abuja, Nigeria, December, 2014

[36] M. J. Edam, H. M. Khadier, S. M. Abdulalmohsin, B. H. Auad, D. E. Tarek, and O. Mushtaq, "Optimum Defect Density of Organic – in Organic for High Efficiency Perovskites Solar Cells," *Int. J. Thin Film. Sci. Technol*., vol. 151, no. 2, pp. 143–151, 2024.

[37] V. M. Goldschmidt, Ber. Dtsch. Chem. Ges. 60 (1927) 1263–1268.

[38] K. Amri, R. Belghouthi, M. Aillerie, and R. Gharbi, "Device optimization of a lead-free perovskite/silicon tandem solar cell with 24.4% power conversion efficiency," Energies, vol. 14, no. 12, 2021, doi: 10.3390/en14123383.

[39] Rahmad, A. Davarpanah, M. K. M. Nasution, Q. Wali, and Dadan Ramdan, "The Effect of Structural Phase Transitions onElectronic and Optical Properties of CsPbI3PureInorganic Perovskites," MDPI, vol. 11, no. 10, p. 720, 2024, doi: 10.3390/coatings11101173.

[40] N. Lakhdar, A. Hima,"Electron transport material effect on performance of perovskite solar cells based on CH3NH3GeI3," *Opt. Mater.* **2020**, *99*, 109517. [CrossRef]

[41] B. Via and N. Simulation, "Optimization of Structure of Solar Cells Based on Lead Perovskites," Sol. Energy Res. (JSER), no. March, 2018.

[42] A. Husainat ,W .Ali ,"Simulation and Analysis of Methylammonium Lead Iodide (CH3NH3PbI3) Perovskite Solar Cell with Au Contact Using SCAPS 1D Simulator," *American Journal of Optics and Photonics*_,Vol 7, Issue 2. August 2019.